LAWRENCE
LIVERMORE
NATIONAL
LABORATORY

UCRL-PROC-216738

Impact of contaminates on the laser damage threshold of 1w HR coatings

M. A. Norton, C. J. Stolz, E.E. Donohue, W. G. Hollingsworth, K. Listiyo, J. A. Pryatel, R. P. Hackel

November 1, 2005

Boulder Damage Symposium XXXVII
Boulder, CO, United States
September 19, 2005 through September 21, 2005

Impact of contaminates on the laser damage threshold of 1ω HR coatings.

Mary A. Norton, Christopher J. Stolz, Eugene E. Donohue, William G. Hollingsworth, Kalvin Listiyo, James A. Pryatel, and Richard P. Hackel

Lawrence Livermore National Laboratory, M/S L592, PO Box 5508, Livermore, CA 94551

ABSTRACT

In operational laser systems, it is often difficult to keep optical components completely free of foreign material. We have investigated the performance of high damage threshold 1.053 μm high reflectors in the presence of surface contaminants. We have looked at the impact of stainless steel, aluminum, Azurlite®, dust, cotton fibers and polyester fibers on the performance of the mirrors under laser irradiation. The first four contaminants were deposited in sizes ranging from 30 microns to 150 microns. The fibers included lengths ranging to several millimeters. The testing was done at either a single fluence in the range of 6 J/cm^2 to 24 J/cm^2, or a ramped sequence of shots starting at 1 J/cm^2. We will present data showing the onset of damage, the type of damage, and the propensity to damage growth in the fluence range studied.

Keywords: Laser damage, laser damage growth, 1 micron high reflectors, particulate contamination.

1. INTRODUCTION

Large laser systems typically contain high reflectors to transport the laser beam both within the amplifier chains and after the final amplifiers. In these laser systems, the mirrors are frequently required to perform at fluences approaching the damage fluence of the mirror coatings themselves both to minimize system costs and to reduce system size. These conditions will make the reflectors vulnerable to reduced damage thresholds due to contaminants that may be inadvertently deposited on the optics. This threat is intensified when the surfaces may be facing upwards.

In spite of careful handling procedures, often foreign matter will be found to settle on transport mirrors.[1] We have considered a suite of materials likely to be the source of particles found near mounted optics in a 1 μm laser system. The materials represent typical mounting hardware materials, glass used for beam dumps, dust collected from a HVAC system in an optics clean room and fibers from materials commonly used found in proximity to optics. This paper will report the results of irradiating high damage threshold HR multilayer dielectric coatings with contaminants of defined sizes.

2. EXPERIMENT

2.1. Experiment layout

Mirror substrates were mounted in air at 45° to the laser beam and oriented at 45° to the horizontal, with the reflecting surface facing up. The test area was viewed with a long working distance microscope. For most of the tests the microscope light source was scattered light from front surface white light illumination. For some of the tests, the microscope derived its signal from the laser interaction with the surface. This allowed the viewing of any plasma that was generated as a result of each laser shot.

The optical layout is shown schematically in figure 1. The fluence of the 25 mm x 25 mm laser beam entering the experiment table is controlled with a half-wave plate and polarizer. The size of the beam is reduced by a single lens with

the part intercepting the beam in the plane where the beam is ~11 mm x 11 mm. A glass beam dump is used directly above the part to intercept the beam before focus. A beam splitter just before the test sample is used to provide a beam sample of the beam on the substrate. This is sent to a calibrated scientific grade CCD camera used to set and monitor the input fluence of each shot. The leak through the mirror is also sent to a CCD camera and is recorded for every shot.

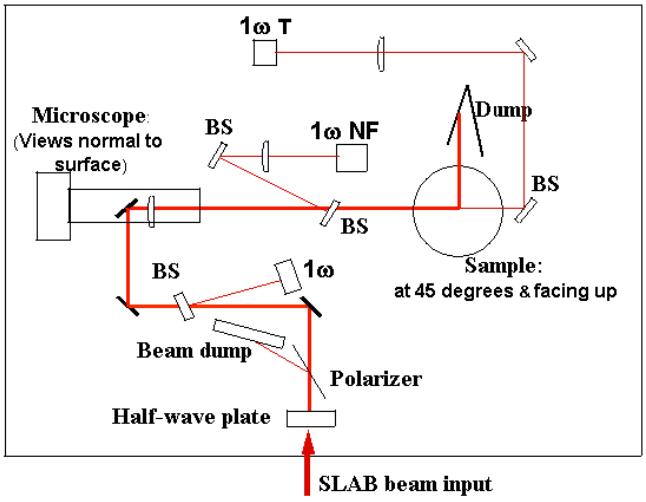

Figure 1. Optical layout.

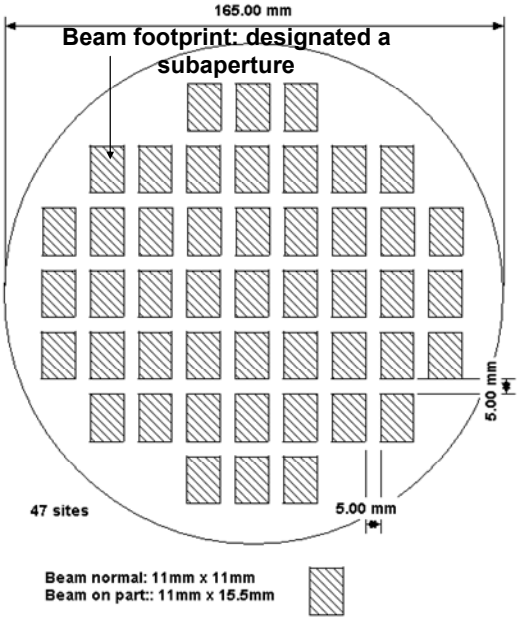

Figure 2. Substrate layout.

2.2. Material details

The mirror substrates are BK7 165-mm diameter and 20 mm thick. The multilayer dielectric coating is a quarter wave hafnia/silica stack. The coating is designed for 45° use angle and a wavelength of 1053 nm. The region of the substrate tested during a test series is called a subaperture and a subaperture covers an area of 11 mm x 15.5 mm. This allowed 27 test areas on one substrate. This layout is shown in figure 2. Three substrates were used during the course of these tests.

The matrix of contaminant materials used for these tests is shown in table 1. The particles were categorized by size: the largest sized particles having diameters in the 90 to 115 µm range, the midsized particles being in the 40 to 55 µm range, and the smallest particles <30 µm range. Two metals, stainless steel and aluminum, were chosen since mounting fixtures frequently employ these metals. There was none of the smallest sized particles for Al. Azurlite®, a copper doped float glass, is useful as a low cost absorber for 1 micron light. The HVAC dust was obtained from the ducts of a clean room where optics are cleaned and mounted. Cotton fibers were obtained from cotton clean room gloves and polyester fibers were obtained from clean room wipes. Polystyrene microspheres were of one fixed diameter: 48 µm.

Material	Size
Stainless steel, 304	<30 µm, 40-55 µm, 90-115 µm
Aluminum, 6061, wrought	40-55 µm, 90-115 µm
Azurlite®	<30 µm, 40-55 µm, 90-115 µm
HVAC dust	<30 µm, 40-55 µm, 90-115 µm
Cotton fiber	20-30 µm diameter, up to 2 mm long
Polyester fiber	20-30 µm diameter, up to 5 mm long
Polystyrene micro-spheres	48 µm diameter

Table 1. Matrix of contaminants.

2.3. Test procedure

Since it has been shown[2] that laser conditioning greatly increases the laser damage threshold of the mirror coatings and the mirrors had not been conditioned, each subaperture was first conditioned. The conditioning of a subaperture was accomplished by setting the average beam peaks to approximately 8 J/cm^2 and increasing the fluence in 0.33 J/cm^2 steps for approximately 50 shots. This typically brought the peaks of the beam footprint to approximately 25 J/cm^2. Then the contaminant was applied and the subaperture shot either with another ramp similar to the conditioning ramp or with a single, fixed fluence for 50 or more shots.

2.4. Laser parameters

The laser system used for these tests is the SLAB laser capable of producing 25 J in a 12 ns pulse of near diffraction limited beam quality at a maximum rep rate of 5 Hz.[3] The beam area normal to the propagation direction as used for these tests is 1.4 cm^2. All fluence values recorded are reported normal to the propagation direction. The actual beam area on the substrate is ~2 cm^2 due to the 45° angle of incidence. The nominal temporal pulse shape has a FWHM of 12.5 ns. When calculating the whole beam average the beam peaks are typically two times the average fluence. The rep rate of the laser used during these tests was 0.3 Hz.

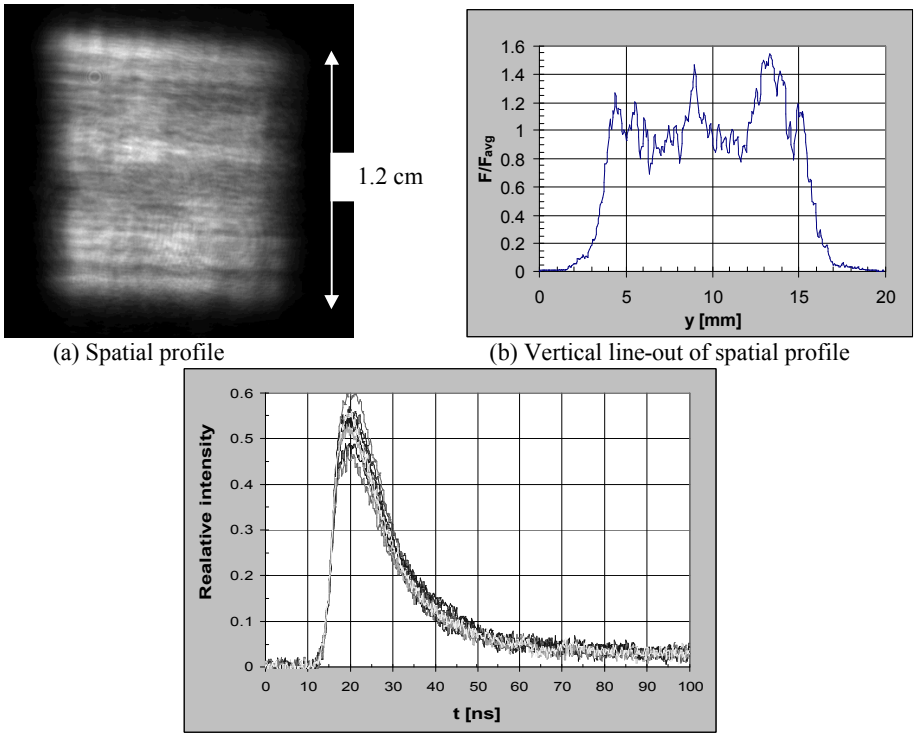

(a) Spatial profile

(b) Vertical line-out of spatial profile

(c) Overlay of 10 temporal waveforms

Figure 3. Typical laser spatial and temporal profiles.

A typical irradiance distribution and typical temporal pulse shapes are shown in figure 3. In figure 3a, the contrast ratio of the central 70% of the beam area is 20%. Figure 3b plots a vertical profile through the beam center and figure 3c is an overlay of the 10 temporal waveforms.

3. EXPERIMENT RESULTS

3.1. Stainless steel particulates

For all three sized particle groups large (>200 μm) damage sites can be initiated when the local fluence exceeds 10 J/cm^2. Once damage is initiated, it can grow if the local fluence exceeds 20 J/cm^2. No large damage sites were initiated for subapertures tested with a ramped fluence sequence.

The 90 to 115 μm particles did not adhere easily, tending to slide off the substrate. Some of these particles were cleaned off the surface during a ramp sequence. Typical initiated damage sites were large (near 500 μm in diameter) and exhibited a characteristic morphology. Figure 4 summarizes the results of shooting a subaperture with the largest particles for 25 shots at an average fluence of 13.6 J/cm^2 ± 2%. Figure 4a is the online microscope image of the starting distribution; figure 4b is taken at the end of the fourth laser shot. Figure 4c is the final image of the subaperture taken after 25 shots with a high resolution offline microscope. Figure 4d is a higher resolution image of the largest damage site. Careful comparisons of the final image with the online images reveal that nearly all the damage occurs within the first few shots and growth may or may not follow after the damage initiates. All of the initiated damage site morphology appears to have a central region with surrounding rings. When growth occurs it starts within the central core and begins eating through the coating. Damage initiated in the regions of the subaperture where the fluence was between 13 and 26 J/cm^2; whereas growth occurred only where the fluence was ~24 J/cm^2. In figure 4d the damage site that grew to over 1 mm in diameter has had the coating eaten through; the smaller site adjacent to this one also shows that the central core region is beginning to be eaten through.

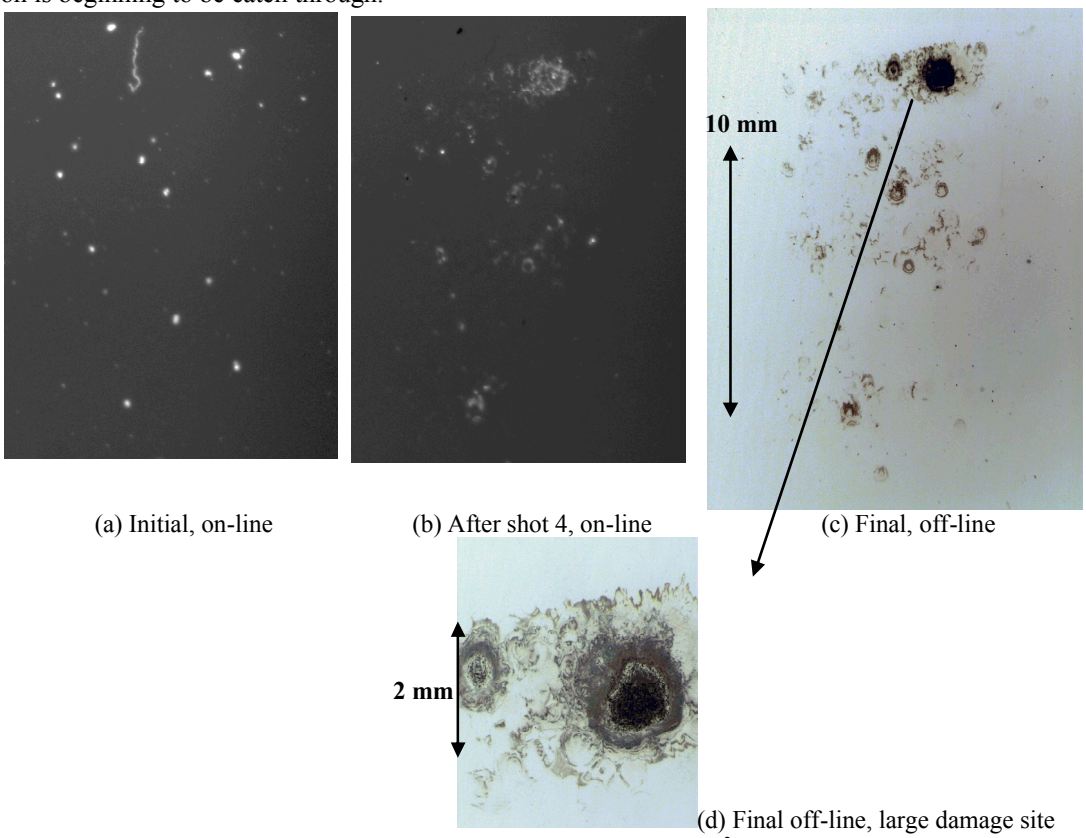

(a) Initial, on-line (b) After shot 4, on-line (c) Final, off-line

(d) Final off-line, large damage site

Figure 4, Microscope images for a subaperture shot at 14 J/cm^2 with 90-115 μm SS particles.

For both the smaller sized stainless steel particle groups, we find the same damage morphology and growth characteristics as seen in figure 4. The fluence needed for initiation and growth is approximately the same. A notable different between the size groups are that the smaller particles adhere more readily and are removed less effectively during the laser ramp shot sequences.

3.2. Aluminum particulates

Both Al size groups tested adhered more readily than the stainless steel counterpart and there was less removal of material noted during the laser ramp shot sequences. Microscope images for a subaperture shot at an average fluence of 10.2 J/cm^2 ± 3% for 70 shots are shown in figure 5.

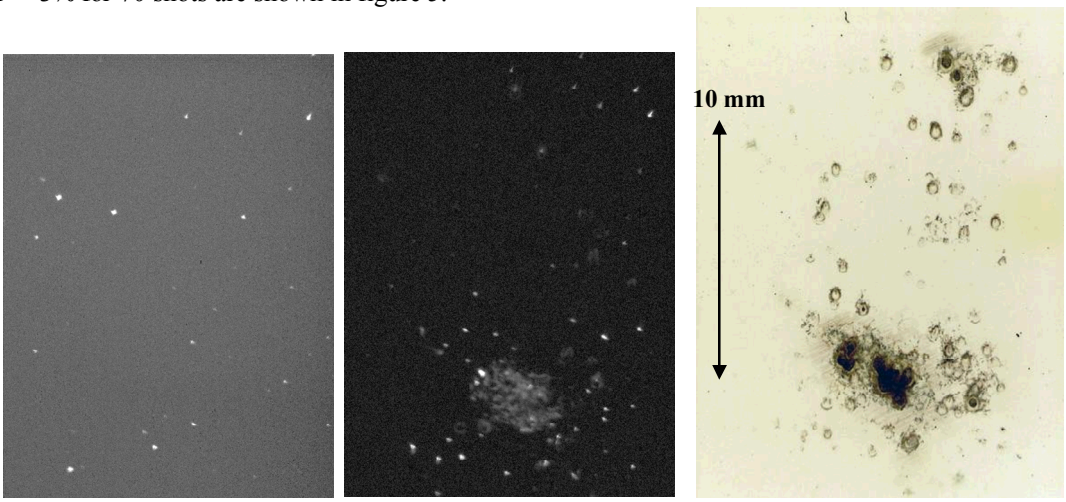

(a) Initial, on-line (b) After shot 10, on-line (c) Final, off-line

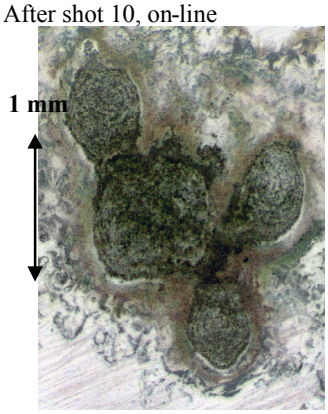

(d) Final large site, off-line

Figure 5. Microscope images for a subaperture shot at 10J/cm^2 with 90-115 μm Al particles.

Figure 5a is the initial particle distribution taken with the on line microscope. A lighter initial density was achieved for the Al particles than for the SS particles. Figure 5b is taken after shot 10. Figure 5c is final off line high resolution image taken after 70 shots; and figure 5d is a magnified image of the heavily damaged region of the subaperture. Just as for the SS case we find that nearly all damage occurs within the first few shots with only some of those located in high fluence areas of the beam showing growth. Many of the initiated damage sites grew for about 10 shots reaching a final diameter of 0.7 to 0.8 mm and then no further changes were observed during the next 50 shots. Al starts damaging at a fluence of ~6 J/cm^2 and also can grow at ~15 J/cm^2. The damage morphology is very similar to SS. Figure 6 includes three images from the online microscope on the same subaperture as shown in figure 5; figure 6a and 6c are before and after the first shot with standard illumination and figure 6b shows an exposure taken with the camera synchronized with the laser pulse and no external light source. Two observations seen in this figure apply to all subapertures shot during these tests. The first observation is that some particles are removed and some particles are deposited in new locations during the initial shots. The arrows on the initial image point to the locations of three particles which were no longer visible after the shot and the arrow in the final picture points to a location having a particle where there was initially no particle visible. The second observation is that damage and growth are accompanied with plasma emission. The middle picture captures emission from plasma ignited by the absorption of laser energy. This plasma emission was observed on all shots where damage or growth occurred.

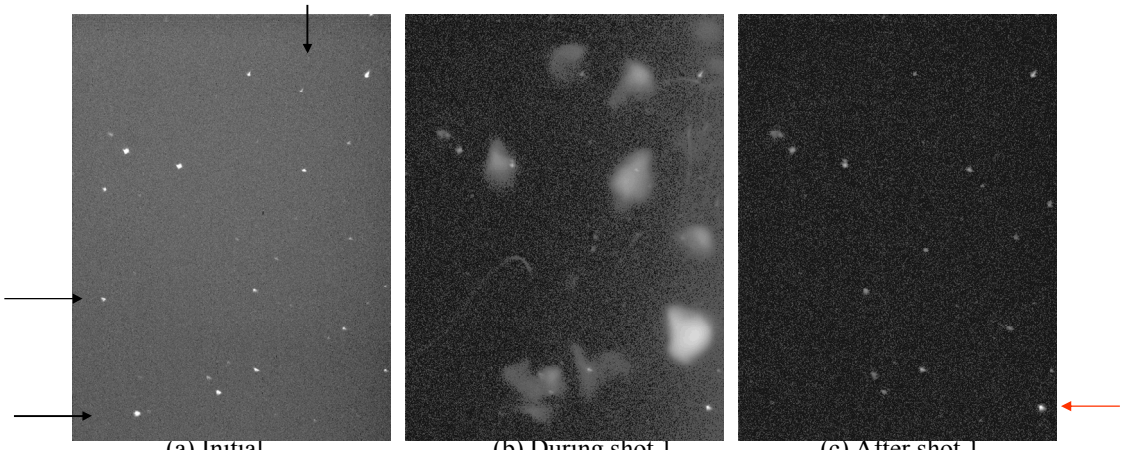

(a) Initial (b) During shot 1 (c) After shot 1

Figure 6. Online microscope images for Al at 10J/cm^2 before, during and after the first shot.

3.3. Azurlite particulates

For all the size groups of Azurlite particles, very little removal was observed during the laser fluence ramp shot sequences. The initiated damage sites did not resemble the morphology of the two metals. The morphology of the initiated damage tended to be small, <100 µm, and found in clusters. All size groups behaved similarly though the largest sized particles appeared to have a slightly higher damage threshold and the smallest particles were less likely to produce damage. Microscope images from a subaperture with particles in the 40-55 µm range are shown in figure 7.

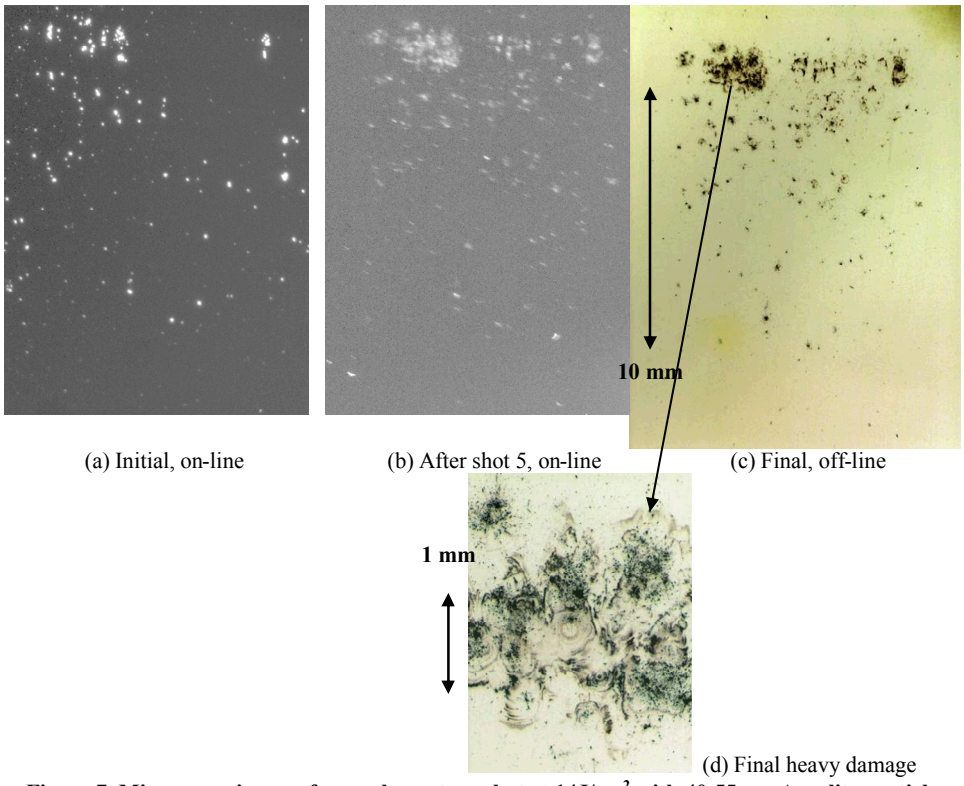

(a) Initial, on-line (b) After shot 5, on-line (c) Final, off-line

(d) Final heavy damage

Figure 7. Microscope images for a subaperture shot at 14J/cm^2 with 40-55 µm Azurlite particles.

This subaperture was shot at an average fluence of 13.8 J/cm^2 ±3% for 200 shots. Figure 7a shows the initial distribution which had a higher concentration in the top half of the subaperture. Figure 7b shows the subaperture after 5 shots, in this case damage initiation continued through a total of 10 shots. Figure 7c shows the final damage density concentrated in the upper portion of the subaperture. Figure 7d shows a magnified image of the most heavily damaged area which the fluence was approximately 25 J/cm^2; here it is seen that there is no severe erosion through the coating as was observed for the metals.

3.4. HVAC dust particles

HVAC particles in all size groups were capable of producing severe damage. In fact, after a heavy initial concentration of the largest particles a single shot 13 J/cm^2 destroyed the coating over the entire subaperture. Figure 8 shows images from a subaperture with an initial concentration of 40-55 μm particles which was shot for only 4 shots at an average fluence of 13.8 J/cm^2.

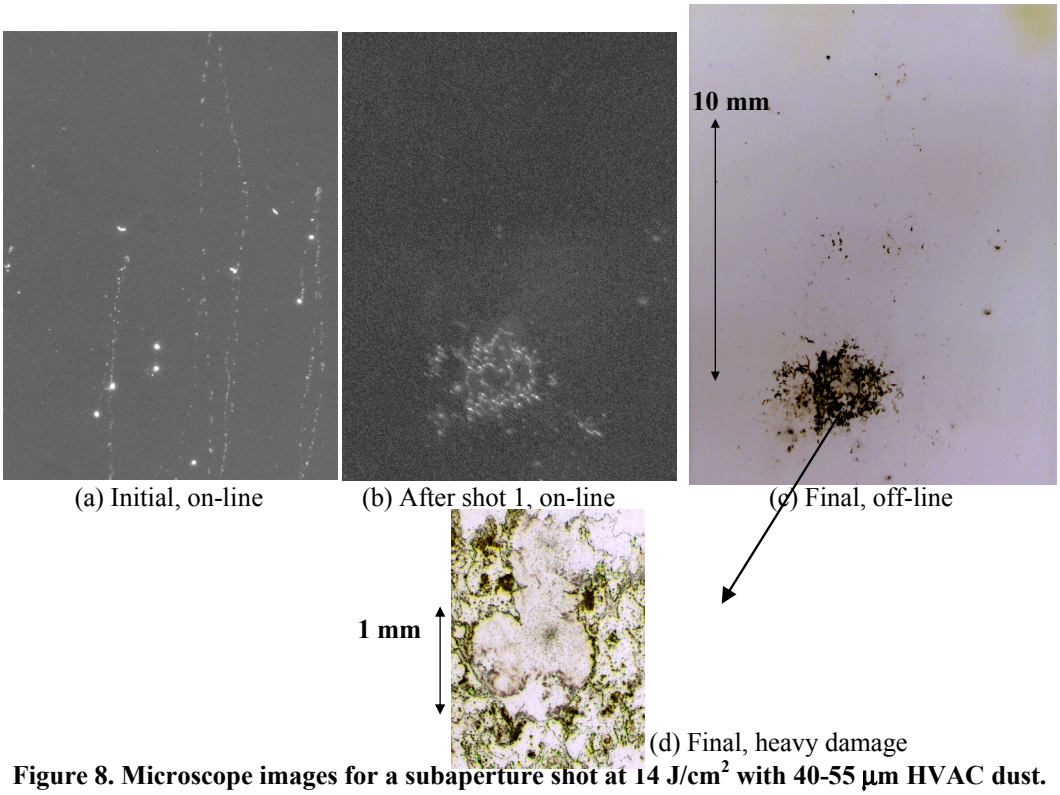

(a) Initial, on-line (b) After shot 1, on-line (c) Final, off-line

(d) Final, heavy damage

Figure 8. Microscope images for a subaperture shot at 14 J/cm^2 with 40-55 μm HVAC dust.

The initial distribution, seen in figure 8a, illustrates what was true for all of the dust subapertures: the dust tends to clump and when dropped onto the surface is the source of a trail of particles. The particles were seen to move in all directions over centimeter length distances as a result of a laser shot. Figure 8b is taken after the second shot and clearly shows that the damage seen in the final image, figure 8c, has formed. Figure 8d, is a magnified image within the damage formed in a 20-25 J/cm^2 region of the subaperture; some erosion of the coating is evident after the 4 shots.

3.5. Fibers and microspheres

The behavior of subapertures shot after depositing cotton and polyester fibers were virtually the same as each other: many small (<100 μm) damage sites were initiated after even the first shot, all fibers were gone after no more than 9 shots and the hottest regions (20 to 25 J/cm^2) of the subapertures induced no growth of the initiated sites in those regions. Figure 9 displays online microscope images from a subaperture shot at 13.9 J/cm^2 ±2% for 100 shots with polyester fibers.

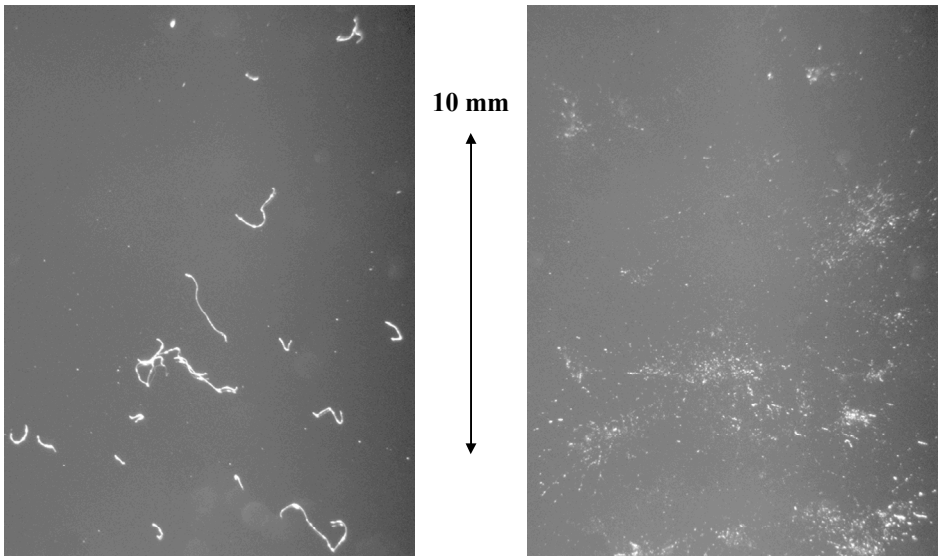

(a) Initial (b) Final

Figure 9. Microscope images of subaperture shot at 14 J/cm^2 with polyester fibers.

Figure 9a shows the initial distribution and figure 9b shows the damage after 100 shots; there were no high resolution images recorded for the fibers. Many small pits were initiated and remained stable after initiation even at a peak fluence of ~25 J/cm^2.

The online microscope images obtained while shooting the polystyrene microspheres for 100 shots at an average fluence of 14 J/cm^2 showed that the spheres were immediately removed and left behind no detectable damage. Careful post inspection has revealed that the subapertures were left with plasma scalds.

4. SUMMARY AND DISCUSSION

The results of shooting all material types and all size groups can be summarized in the graph shown in figure 10.

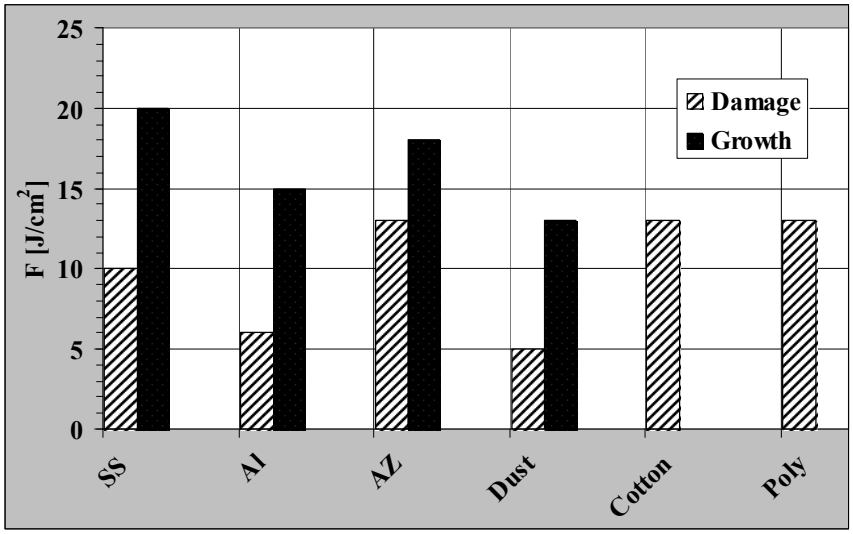

Figure 10. Thresholds for damage and growth for all particulates.

The plot does not distinguish between size groups for a given material because it was predominately the type of material and not the size that determined the behavior. Thus all the materials tested are a damage threat when the fluence is >5 J/cm^2. Azurlite and the fibers do not produce damage until the fluence reaches 18 J/cm^2. Al has the lowest threshold

both for damage initiation and damage growth: 5 J/cm^2 and 15 J/cm^2 respectively. Growth in diameter of SS and Al initiated damage appears to be linear with shot number but growth frequently leveled off after 10 shots. As an example of a site that did not level off, we found an increase of ~15 μm/shot at 25 J/cm^2 for an initiated damage site for the large sized Al particles. For both fiber types, we did not find a growth threshold; if this damage will grow the threshold is apparently >25 J/cm^2. For the microspheres, we found neither a damage nor a growth threshold; we assume they are both >25 J/cm^2, if indeed they are capable of causing damage at fluence levels below the damage threshold of the coating itself.

We have found that the damage morphology for both metals is similar: large, with a central region surrounded by a ring-like structure. Azurlite damage tends to be small pits, leaving a rough surface. HVAC dust tends to produce clusters of small pits which are prone to growth. Fibers also produce small pits which tend to cluster. Most particles can initiate damage that will grow to 1 mm in 10 shots at 25 J/cm^2.

The HVAC dust was not analyzed for its chemical composition. Due to its observed deleterious effects on the coating further investigation needs to be completed to identify the source of the low damage threshold.

The observations of particle removal during the testing of subapertures that were ramped from low to high fluence suggest that a "laser cleaning" protocol might be developed to avoid laser damage from particle contamination. Though we observed that particles were removed, we did no post testing to determine if a deleterious effect occurred on the reflecting properties of the coatings. Thus further testing is required to establish the viability of the laser itself as a tool to avoid damage.

From the test results reported here, it is important to keep transport mirrors free of all of the contaminants investigated for operations having peak fluences exceeding 15 J/cm^2.

---

[1] W. H. Gourdin, E. Dzenitis, D. Martin, K. Listiyo, G. Sherman, W. Kent, R. Butlin, C. J. Stolz and J. Pryatel, "*In-situ* surface debris inspection and removal system for upward-facing transport mirrors of the National Ignition Facility", *Proc. SPIE* 5647, 107, 2004.

[2] A. B. Papandrew, C. J. Stolz, Z. L. Wu, G. E. Loomis, and S. Flabella, "Laser conditioning characterization and damage threshold prediction of hafnia/silica multilayer mirrors by photothermal microscopy", *Proc. SPIE* 4347, 53, 2000.

[3] C. B. Dane, L. E. Zapata. W. A. Neuman, M. A. Norton, and L. A. Hackel, "Design and Operation of a 150 W Near Diffraction-limited Laser Amplifier with SBS Wavefront Correction," *IEEE J. Quantum Electronics*, **31**, pp. 148-163, 1995.

This work was performed under the auspices of the U.S. Department of Energy by the University of California, Lawrence Livermore National Laboratory under Contract No. W-7405-Eng-48.